Proc. Natl. Acad. Sci. USA
Vol. 93, pp. 8826–8829, August 1996
Applied Biological Sciences

Direct atomic force microscope imaging of *Eco*RI endonuclease site specifically bound to plasmid DNA molecules

D. P. ALLISON*†, P. S. KERPER*, M. J. DOKTYCZ*, J. A. SPAIN*, P. MODRICH‡, F. W. LARIMER§, T. THUNDAT*, AND R. J. WARMACK*

*Health Sciences Research Division and §Biology Division, Oak Ridge National Laboratory, Oak Ridge, TN 37831-6123; and ‡Department of Biochemistry, Duke University Medical Center, Durham, NC 27710

Communicated by Oscar L. Miller, Jr., University of Virginia, Charlottesville, VA, May 10, 1996 (received for review November 6, 1995)

ABSTRACT **Direct imaging with the atomic force microscope has been used to identify specific nucleotide sequences in plasmid DNA molecules. This was accomplished using *Eco*RI(Gln-111), a mutant of the restriction enzyme that has a 1000-fold greater binding affinity than the wild-type enzyme but with cleavage rate constants reduced by a factor of 10^4. *Sca*I-linearized plasmids with single (pBS$^+$) and double (pGEM-*luc* and pSV-β-galactosidase) *Eco*RI recognition sites were imaged, and the bound enzyme was localized to a 50- to 100-nt resolution. The high affinity for the *Eco*RI binding site exhibited by this mutant endonuclease, coupled with an observed low level of nonspecific binding, should prove valuable for physically mapping large DNA clones by direct atomic force microscope imaging.**

Restriction endonucleases are enzymes that recognize and bind to specific nucleotide sequences resulting in cleavage of the DNA molecule. The frequency with which these enzymes cleave DNA is determined by both the number and order of nucleotides in the recognition site. Since each position in a specific sequence can be occupied by one of four possible nucleotides, an endonuclease that recognizes a specific sequence of 3 nt would be expected to cleave DNA every 64 bases while an enzyme that is site specific for a 6-nt sequence would cleave DNA, on the average, every 4096 bases. Because restriction enzymes are site specific, their attachment sites can serve as physical map points along DNA molecules.

Conventional methods for locating the restriction sites, for a specific endonuclease, rely on cutting the DNA molecules into fragments. Ordering of the fragments and consequent identification of the restriction sites is typically accomplished by a combination of techniques that include multiple partial endonuclease digestion, gel fractionation, Southern blot analysis, and hybridization with labeled end probes (1). As the number of restriction sites to be identified and, therefore, the molecular length of the DNA increases, ordering the restriction sites becomes more difficult. For example, locating the expected 8–15 *Eco*RI or *Bam*HI sites on a 100-kb cloned DNA would require roughly a month's work and may be compromised by the presence of rapidly cleaved recognition sites.

An alternative to identifying restriction sites by fragment analysis would be to use microscopy to image restriction sites on intact DNA molecules. Enzymes such as RNA polymerase (2–4), wild-type *Eco*RI endonuclease (5), and other proteins (6) bound to short pieces of DNA have been imaged by the atomic force microscope (AFM). Also, a site-specific antibody for Z-DNA sequences bound to a plasmid has been imaged (7). However, imaging the relatively small *Eco*RI endonuclease site specifically bound to long DNA molecules is more challenging due to the small size of the protein that may be confused with background noise, especially when large areas are imaged.

*Eco*RI is a dimeric globular protein of known sequence with a molecular weight of 62,000. The nucleic acid recognition site is GAATTC and the two monomeric subunits of the dimeric endonuclease bind to this site and the complementary site on duplex DNA molecules (8, 9). Identifying the binding site on intact DNA molecules requires that the enzyme bind but not cut the molecule. This can be accomplished by using Gln-111 a mutant *Eco*RI endonuclease modified to bind but not cleave DNA (10). In this study we have identified, by imaging with the AFM, both single and double *Eco*RI sites on linearized plasmid molecules. We anticipate that this technique can be extended to directly image *Eco*RI endonuclease specifically bound to multiple sites on 50-kb DNA molecules. When fully developed this direct imaging technique could be used to rapidly map cosmid-sized clones at a great savings of time over conventional methods.

METHODS

The plasmids used in this study were pBS$^+$ (3204 bp, from Stratagene) with one *Eco*RI site, and pGEM-*luc* (4933 bp, from Promega) and pSV-β-galactosidase (6821 bp, from Promega) with two *Eco*RI sites. Plasmids were linearized with *Sca*I (Life Technologies, Gaithersburg, MD) using the protocol suggested by the manufacturer, phenol/chloroform-extracted, ethanol-precipitated, and resuspended in 10 mM Tris·HCl/1.0 mM EDTA (TE) at pH 7.5 to a final concentration of 200–400 μg/ml (11). Both wild-type *Eco*RI endonuclease (Life Technologies, Gaithersburg, MD) and a genetically engineered mutant having Gln substituted for Glu at position 111 in the amino acid sequence were used in these studies. The consequence of this mutation is that the rate constants for first and second strand cleavage are reduced by a factor of 10^4 while the specific affinity of the Gln mutant for *Eco*RI sites is 1000 × greater than that of the wild-type endonuclease (10, 12).

Binding of the Gln-111 mutant to linearized plasmid DNA was accomplished by incubating, at 37°C, a 20- to 50-fold molar excess of enzyme with 0.1–0.2 μg of plasmid in 20 μl of 100 mM NaCl/12 mM $Mg(OAc)_2$/10 mM potassium phosphate, pH 7.5 (binding buffer). This buffer and other parameters, including incubation time and enzyme-to-plasmid concentration, were evaluated and determined by incubating the Gln-111 enzyme with pBS$^+$ (one *Eco*RI site) for 15 min followed by a 50-fold excess of wild-type *Eco*RI. Results were analyzed on 1.2% agarose gels, with ethidium bromide, and the conditions affording the maximum protection from *Eco*RI cleavage were selected.

To ensure proper surface coverage for AFM imaging, the 20-μl plasmid-Gln-111 samples were diluted 1:5, 1:10, and 1:20 in binding buffer. A 25-μl aliquot of sample was pipetted onto

The publication costs of this article were defrayed in part by page charge payment. This article must therefore be hereby marked "*advertisement*" in accordance with 18 U.S.C. §1734 solely to indicate this fact.

Abbreviation: AFM, atomic force microscope.

†To whom reprint requests should be addressed.

several freshly cleaved 3/8-inch diameter mica disks (1 inch = 2.54 cm). After 5 min the disks were rinsed by plunging 10 times into deionized distilled H_2O, rinsed with a stream of deionized distilled water, rinsed by plunging 10 times into 1:1 H_2O/EtOH, and then rinsed three times in 100% EtOH, the last of which is critical-point-dried (13). We have found that this step greatly reduces surface contamination making imaging of large DNA molecules routine and similiar to results obtained with the electron microscope does not interfere with the imaging of DNA–protein complexes (14).

After drying, the samples were imaged with a Nanoscope II AFM (Digital Instruments, Santa Barbara, CA) operated in the constant force mode (1.5–3 nN) using 200-μm cantilevers with a spring constant of 0.12 N/m (Nanoprobes, Digital Instruments, Santa Barbara, CA). Images were taken at a scan rate of 2.85 Hz with an information density of 400 × 400 points. Since contrast and width of DNA images are affected by both friction and relative humidity, the direction of scans was rotated to minimize frictional effects (15). The effects of humidity were minimized by placing the AFM in a enclosed environmental chamber where the humidity was maintained below 15% by purging with dry nitrogen. All images are presented as flattened raw data.

The accuracy of the dimensional measurements made was checked by calibrating the AFM scanner using a calibration grating supplied by the manufacturer. Length measurements were obtained from images using digital analysis software (NIHIMAGE, National Institutes of Health).

RESULTS AND DISCUSSION

Unlike the scanning tunneling microscope (STM), where molecular conductivity is necessary for imaging and DNA molecules must be anchored to mounting surfaces to prevent being removed by forces exerted by the probe tip (16–18), DNA can be adsorbed to untreated mica surfaces and imaged by AFM (19, 20). However, using this extremely simple procedure for preparing samples causes molecules to undergo drying stress producing supertwisting of molecules making contour measurements difficult. By treating the mica surface with Mg^{2+} (21) or with Ba^{2+} (22) or Co^{2+} (23), DNA can be applied to the surface with good results and reliable length measurements of DNA can be made. Recently, it was found that by simply adding Mg^{2+} to the DNA solution prior to mounting on mica gave good results and that by adding Ni^{2+} (24) to the mounting buffer allowed DNA to adhere to the mica with sufficient strength to be imaged under liquid by AFM.

Buffer conditions for optimal binding of Gln-111 to DNA were evaluated by incubating the mutant enzyme with linearized pBS$^+$ plasmid, followed by digestion with wild-type *Eco*RI and gel electrophoresis. If the mutant enzyme was bound to the recognition site the wild-type *Eco*RI would not cleave the plasmid. A typical result using the binding buffer (100 mM NaCl/12 mM $Mg(OAc)_2$/10 mM potassium phosphate at pH 7.5) is shown in Fig. 1. It can be clearly seen that *Eco*RI cuts the plasmid (lane 2), while incubating the plasmid with the Gln-111 mutant clearly protects the plasmid from *Eco*RI digestion (lane 3). In lanes 4 and 5, the NaCl component was left out of the binding buffer and protection from *Eco*RI digestion by Gln-111 bound to the active site (lane 5) is decreased. We also found in the course of these experiments that lowering the concentration of $Mg(OAc)_2$ in the binding buffer also significantly decreased the amount of DNA protected from *Eco*RI digestion.

Concurrent with developing optimal binding conditions for the mutant endonuclease to the *Eco*RI site on pBS$^+$ plasmid, AFM image quality was evaluated for the different buffer conditions tested. Since the AFM produces images by mechanically tracing the surface, adsorbates on either the mounting substrate or the sample will be reproduced. Therefore, sample mounting solutions were selected that minimized both surface and sample contamination with buffer salts. This becomes critical when considering what contribution the bound protein should make to the image. Crystallographic analysis of the *Eco*RI–DNA complex shows a globular structure 5 nm in diameter at the binding site, which is 2.5 times the 2-nm molecular width of duplex DNA alone (25). From previous AFM studies where the probe tip was modeled as a hemisphere with radius R and the DNA as a cylinder with radius r, the expected width of DNA imaged by AFM can be calculated as $4(Rr)^{1/2}$ (26). Using commercial tips, Nanoprobes, with a radius of curvature of around 12 nm, the calculated imaged width of DNA should be about 14 nm. Depending on the quality of the tip, this is in agreement with observed imaged widths of 9–15 nm. If the DNA is complexed with the mutant *Eco*RI endonuclease, the actual increase in width, from crystallographic measurements, is from 2 to 5 nm or 2.5 times. However, if the globular DNA–*Eco*RI complex is modeled as a cylinder or a sphere with a 2.5-nm radius, the calculated width that should be imaged by AFM is 22 nm, which is an increase in width of only 60% over the 14-nm width calculated for DNA imaged alone. Nevertheless, by experimentally choosing the optimal

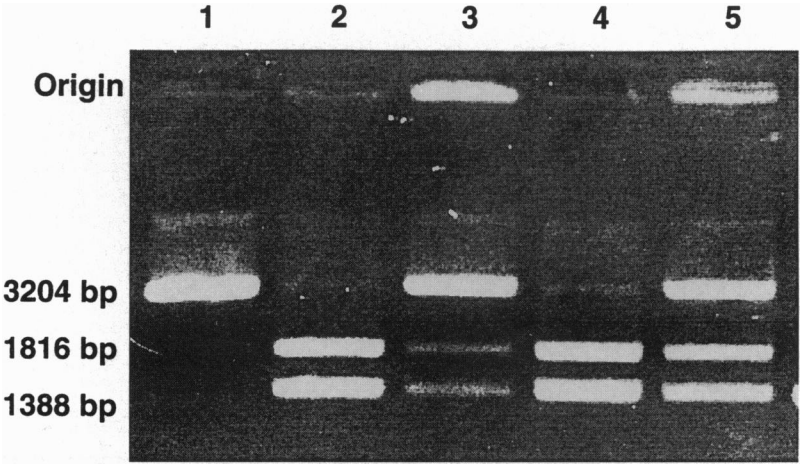

FIG. 1. Specific-site protection by Gln-111 from cleavage by wild-type *Eco*RI endonuclease. In lanes 1–3 *Sca*I-linearized pBS$^+$ plasmid was diluted into the binding buffer (100 mM NaCl/12 mM $Mg(OAc)_2$/10 mM potassium phosphate at pH 7.5). Lanes: 1, pBS$^+$ only; 2, pBS$^+$ and *Eco*RI; 3, *p*BS$^+$ incubated with Gln-111 prior to adding *Eco*RI. In lanes 4 and 5, NaCl was omitted from the binding buffer. Lanes: 4, pBS$^+$ and *Eco*RI; 5, pBS$^+$ incubated with Gln-111 prior to adding *Eco*RI.

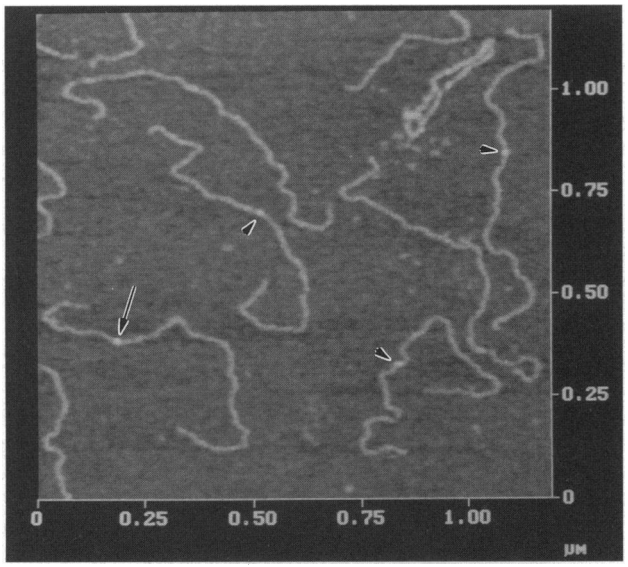

FIG. 2. Contact-mode AFM image of a field of *Sca*I-linearized pBS$^+$ plasmid molecules with three of the molecules site specifically complexed with the mutant *Eco*RI endonuclease (arrowheads). The *Eco*RI site on the linearized plasmid is located 1388 bp from one end of the 3204-bp molecule. Note that in one DNA molecule, which is rarely found, the enzyme is not site specifically bound (arrow).

sample preparation procedures, followed by thoroughly rinsing after mounting and critical point drying, the endonuclease–DNA complex can be imaged by AFM. In the AFM image in Fig. 2 site-specific binding is apparent where three of the several *Sca*I-linearized pBS$^+$ plasmids in the field show the enzyme asymmetrically bound to the 3204-bp plasmid 1388 bp from the *Sca*I cleavage site. One other molecule in this image also clearly shows the enzyme nonspecifically bound to the plasmid, a condition that we rarely observe.

All of the plasmids used in this study are well characterized with respect to molecular length and position of restriction enzyme sites. In Fig. 3, maps of the *Sca*I-linearized plasmids are shown with their known molecular lengths and the position of *Eco*RI restriction sites are given in both base pair and nanometer lengths of fragments, assuming that the molecules are in the B form of DNA with 0.34-nm interbase distance (1). The experimental results are in parentheses in Fig. 3, while images of the linearized plasmids complexed with Gln-111 are presented in Fig. 4. Numerical data was the result of at least 20 molecules of each plasmid being imaged (actual numbers are given in the figure legend) and measured.

These results show that the identification of site-specific binding of enzymes to DNA molecules visualized by direct AFM imaging is accurate to about 100 bp. It should also be noted that no attempt was made to normalize the data. For example, tip convolution that contributes to making the 2 nm width of DNA be imaged as a 9- to 15-nm wide molecule should also add a half width to each end of an imaged DNA molecule. From our experimental results, all of the plasmids were imaged slightly longer than their known molecular lengths, therefore, adding credibility to this argument. However, in all three plasmids measured one of the fragments from an *Eco*RI site to the end of the molecule measured longer than expected while the other *Eco*RI site to the other molecular end was shorter. Images presented in Fig. 4 clearly show that imaging site-specific binding of proteins to DNA molecules is feasible. Although the calculated increase in height and width of the *Eco*RI–DNA complex should only be about 60% greater than DNA alone, which is what we observe, by exploiting differences in height bound enzyme can be readily identified. All of the images in Fig. 4 were taken at the same height scale, included in Fig. 4*A*, of 0–4 nm from dark (low) to light (high). So the DNA molecule bound to the mounting surface will appear lighter than the background and the bound enzyme will appear as a bright spot on the DNA molecule.The three plasmids imaged were chosen for their degree of complexity with the relatively small pBS$^+$ plasmid with one *Eco*RI site being the simplest and pSV-β-galactosidase with two *Eco*RI sites being the largest and, therefore, the most complex. Successful imaging is accomplished when the contribution of background contamination is minimize and contamination of DNA by precipitated or adsorbed salts is effectively eliminated. Another encouraging aspect of these results is that samples can be prepared and imaged with at least 20–30 molecules statistically analyzed in a day. We have also found that larger molecules such as bacteriophage λ DNA (48 kb) can be imaged although only five or so good images can be accomplished in a day. This is because as the length of the molecule increases the probability of the molecule becoming entangled with itself or with other molecules becomes a problem, making accurate measurements difficult. Nevertheless, demonstrated success in imaging both *Eco*RI site-

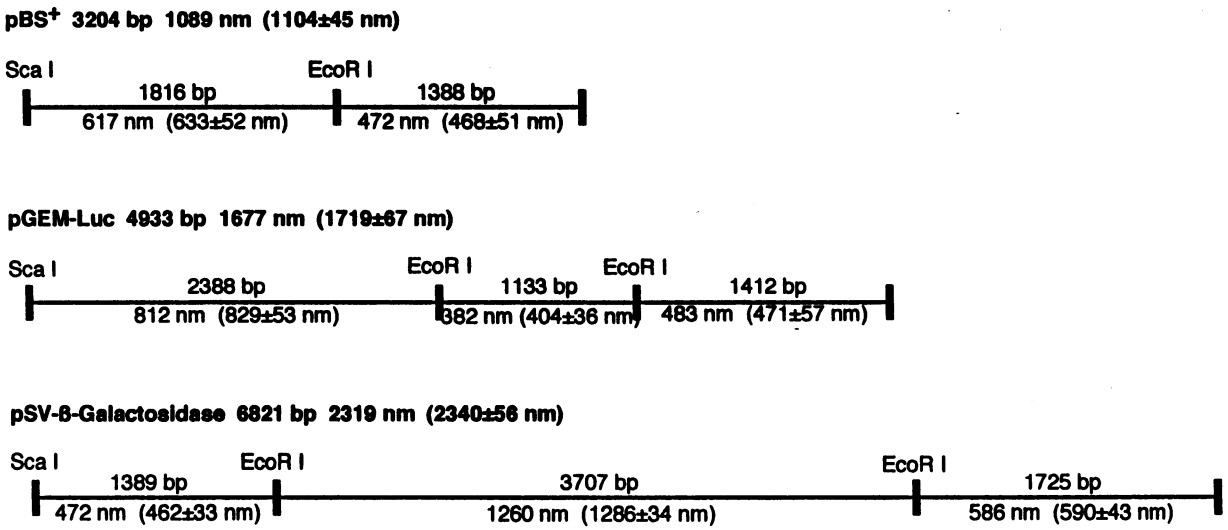

FIG. 3. *Sca*I-linearize plasmids are drawn to scale with the known distances given in both base pairs and nanometers. The experimental data are presented within parenthesis with distances and standard deviation given in nanometers. The number of molecules measured were 26 pBS$^+$, 24 pGEM-*luc*, and 25 pSV-β-galactosidase.

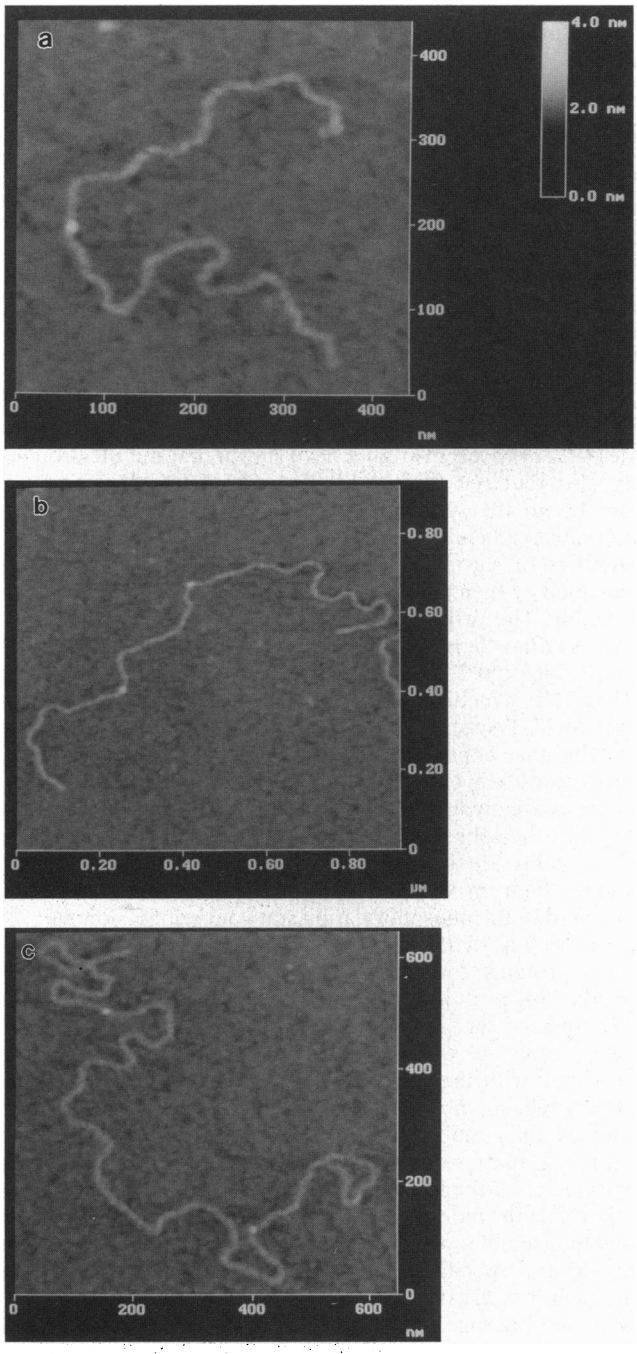

FIG. 4. Contact-mode AFM images of all of the plasmids clearly show the mutant *Eco*RI endonuclease site specifically bound. Height information contained in the 0- to 4-nm scale (gray scale), included in *a*, is used to facilitate identification of the bound enzyme. All of the images in the figure are taken at the same height scale where dark is low and light is high. Therefore, DNA molecules will appear lighter than the mounting substrate and the bound enzyme that adds extra dimension will be imaged as a distinct light spot. The smallest plasmid pBS$^+$ (*a*) imaged at the highest magnification shows the best resolution of Gln-111 bound to its single *Eco*RI site. The two sites on pGEM-*luc* (*b*) when compared with the map in Fig. 3 again show the mutant endonuclease bound to the plasmid in the correct position, while in *c* the two *Eco*RI sites near the ends of the linearized pSV-β-galactosidase plasmid are clearly identified by the bound mutant enzyme.

specifically bound to plasmid molecules and in imaging large cosmid sized DNA molecules encourages the development of this technology for mapping genomic DNA by direct AFM imaging.

CONCLUSION

The experimental results show that it is possible to image, with the AFM, the site-specific binding of mutant *Eco*RI endonuclease to plasmid molecules. Furthermore, 50- to 100-base resolution makes this an extremely accurate technique for defining distances between restriction sites. Future experimental efforts should be focused on applying this technique to mapping 50-kb cosmid-sized molecules. If successful this technology should be fully transferable to laboratories doing genomic mapping and has the potential to *Eco*RI map, at high resolution, large insert clones, at a great savings of time over conventional mapping techniques.

This research is sponsored by the U.S. Department of Energy under Contract DE-AC05-96OR22464 with Oak Ridge National Laboratory, managed by Lockheed Martin Energy Research.

1. Watson, J. D., Hopkins, N. H., Roberts, J. W., Seitz, J. A. & Weiner, A. M. (1988) *Molecular Biology of the Gene* (Benjamin/Cummings, Menlo Park, CA), p. 249.
2. Bustamante, C., Vesenka, J., Tang, C. L., Rees, W., Guthold, M. & Keller, R. (1992) *Biochemistry* **31,** 22–26.
3. Zenhausern, F., Adrian, M., Tenhieggeler-Bordier, B., Eng, L. M. & Descouts, P. (1992) *Scanning* **14,** 212–217.
4. Hansma, H. G., Bezanilla, M., Zenhausern, F., Adrian, M. & Sinsheimer, R. L. (1993) *Nucleic Acids Res.* **21,** 505–512.
5. Niu, L., Shaiu, W.-L., Vesenka, J., Larson, D. D. & Henderson, E. (1993) *SPIE Proc.* **1891,** 71–77.
6. Erie, D. A., Yang, G., Schultz, H. C. & Bustamante, C. (1994) *Science* **266,** 1562–1566.
7. Pietrasanta, L. I., Schaper, A. & Jovin, T. M. (1994) *Nucleic Acids Res.* **22,** 3288–3292.
8. Greene, P. J., Gupta, M., Boyer, H. W., Brown, W. E. & Rosenberg, J. M. (1981) *J. Biol. Chem.* **256,** 2143–2153.
9. Newman, A. K., Rubin, R. A., Kim, S.-H. & Modrich, P. (1981) *J. Biol. Chem.* **256,** 2131–2139.
10. Wright, D. J., King, K. & Modrich, P. (1989) *J. Biol. Chem.* **264,** 11816–11821.
11. Sambrook, J., Fritsch, E. F. & Maniatis, T. (1989) *Molecular Cloning: A Laboratory Manual* (Cold Spring Harbor Lab. Press, Plainfield, NY), 2nd Ed.
12. Terry, B. J., Jack, W. E. & Modrich, P. (1985) *J. Biol. Chem.* **260,** 13130–13137.
13. Thundat, T., Warmack, R. J., Allison, D. P. & Jacobson, K. B. (1994) *Scanning Microsc.* **8,** 23–30.
14. Griffith, J. D. (1973) *Methods Cell Biol.* **7,** 129–156.
15. Thundat, T., Warmack, R. J., Allison, D. P., Bottomley, L. A., Lourenco, A. J. & Ferrell, T. L. (1992) *J. Vac. Sci. Technol. A* **10,** 630–635.
16. Lyubchenko, Y. L., Lindsay, S. M., DeRose, J. A. & Thundat, T. (1991) *J. Vac. Sci. Technol. B* **9,** 1288–1290.
17. Lindsay, S. M. & Barris, B. (1988) *J. Vac. Sci. Technol. A* **6,** 544–547.
18. Allison, D. P., Thundat, T., Jacobson, K. B., Bottomley, L. A. & Warmack, R. J. (1993) *J. Vac. Sci. Technol. A* **11,** 816–819.
19. Henderson, E. (1992) *Nucleic Acids Res.* **20,** 445–447.
20. Thundat, T., Allison, D. P., Warmack, R. J. & Ferrell, T. L. (1992) *Ultramicroscopy* **42-44,** 1101–1106.
21. Vesenka, J., Guthold, M., Tang, C. L., Keller, D., Delaine, E. & Bustamante, C. (1992) *Ultramicroscopy* **42-44,** 1243–1249.
22. Thundat, T., Allison, D. P., Warmack, R. J., Doktycz, M. J., Jacobsen, K. B. & Brown, G. M. (1993) *J. Vac. Sci. Technol. A* **11,** 824–828.
23. Thundat, T., Allison, D. P., Warmack, R. J., Brown, G. M., Jacobson, K. B., Schrick, J. J. & Ferrell, T. L. (1992) *Scanning Microsc.* **6,** 911–918.
24. Bezanilla, M., Drake, B., Nudler, E., Kashlev, M., Hansma, P. K. & Hansma, H. (1994) *Biophys. J.* **67,** 2454–2459.
25. McClarin, J. A., Frederick, C. A., Wang, B.-C., Greene, P., Boyer, H. W., Grable, J. & Rosenberg, J. M. (1986) *Science* **234,** 1526–1541.
26. Thundat, T., Zheng, X.-Z., Sharp, S. L., Allison, D. P., Warmack, R. J., Joy, D. C. & Ferrell, T. L. (1992) *Scanning Microsc.* **6,** 903–910.